

β -Ga₂O₃ MOSFETs with near 50 GHz f_{MAX} and 5.4 MV/cm average breakdown field

Chinmoy Nath Saha, Abhishek Vaidya, A F M Anhar Uddin Bhuiyan, Lingyu Meng, Hongping Zhao, Senior Member, IEEE and Uttam Singiseti Senior Member, IEEE

Abstract—This letter reports high-performance β -Ga₂O₃ thin channel MOSFETs with T-gate and degenerately doped source/drain contacts regrown by MOCVD. Gate length scaling ($L_G = 160$ -200 nm) leads to a peak drain current ($I_{D,\text{MAX}}$) of 285 mA/mm and peak trans-conductance (g_m) of 52 mS/mm at 10 V drain bias with 23.5 Ω mm on resistance (R_{on}). A low metal/n+ contact resistance of 0.078 Ω mm was extracted from TLM measurement. R_{on} is dominated by interface resistance between channel and regrown layer. A gate-to-drain breakdown voltage of 192 V is measured for $L_{\text{GD}} = 355$ nm resulting in average breakdown field (E_{AVG}) of 5.4 MV/cm. This E_{AVG} is the highest reported among all sub-micron gate length lateral FETs. RF measurements on 200 nm Silicon Nitride (Si₃N₄) passivated device shows a current gain cut off frequency (f_T) of 11 GHz and record power gain cut off frequency (f_{MAX}) of 48 GHz. The $f_T \cdot V_{\text{BR}}$ product is 2.11 THz.V for 192 V breakdown voltage. The switching figure of merit exceeds that of silicon and is comparable to mature wide-band gap devices.

Index Terms—Ga₂O₃, power gain cut off frequency, switching figure of merit.

I. INTRODUCTION

β -Ga₂O₃ has attracted intense attention worldwide because of its favourable material properties [1] for power, RF switching and RF applications [1], [2]. Multi-kV drain breakdown voltages have been reported in FETs [3]–[6] and diodes [7]–[9]. Theoretically calculated large electron saturation velocity [10] also makes Ga₂O₃ a suitable candidate for next generation RF transistors. Mature bulk crystal growth [11] and thin film growth techniques (MOCVD, MBE, HVPE) with controllable doping (10^{16} - 10^{20} cm⁻³) [12]–[15] have made device fabrication with novel structures possible including both depletion and enhancement mode FETs. [16]–[19]. Modulation doped β -(Al_xGa_{1-x})₂O₃/Ga₂O₃ Heterostructure FET (HFET) have been demonstrated with record 30/37 GHz f_T/f_{MAX} [20] and high temperature stability of RF performance up to 250°C [21] Highly doped contact regrowth process using MOCVD and MBE have been reported with very low contact resistance

We acknowledge the support from AFOSR under award FA9550-18-1-0479 (Program Manager: Ali Sayir), from NSF under awards ECCS 2019749, ECCS 1919798, from Semiconductor Research Corporation under GRC Task ID 3007.001, and II-VI Foundation Block Gift Program.

Chinmoy Nath Saha, Abhishek Vaidya and Uttam Singiseti are with Electrical Engineering department, University at Buffalo, Buffalo, NY-14260, USA.

A F M Anhar Uddin Bhuiyan, Lingyu Meng, Hongping Zhao are with Department of Electrical and Computer Engineering, The Ohio State University, Columbus, OH 43210, USA

[22], improved g_m and RF performance in MESFETs [23] and AlGaO/GaO HFETs [20], [24]. Thick channel (≥ 200 nm) β -Ga₂O₃ MOSFET has been demonstrated but poor gate control because of thicker channel degrades high frequency performances [25]–[27].

In this letter, we report a highly scaled T gate β -Ga₂O₃ thin channel MOSFET for achieving better gate control and improved RF performance. We demonstrate devices with simultaneously high $I_{D,\text{max}}$ (>250 mA/mm) with low R_{on} (<25 Ω mm), high average field strength E_{AVG} (>4.5 MV/cm) and $f_T, f_{\text{MAX}} >10$ GHz. The device showed a highest f_{MAX} of 48 GHz among Ga₂O₃ FETs. We demonstrated high average breakdown field without any field plate technique which could potentially provide cost advantages for high voltage RF applications.

II. DEVICE STRUCTURE AND FABRICATION

The epitaxial structure of the device was grown on (010) Fe-doped semi-insulating Ga₂O₃ substrate using ozone molecular beam epitaxy (MBE) method following conditions described in ref. [28]. The device stack consists of 200 nm unintentionally (UID) doped buffer layer and 60 nm Si doped (9.2×10^{17} cm⁻³) channel. Device fabrication started with blanket ALD Al₂O₃, PECVD SiO₂ and e-beam evaporated Cr layers. Next, using Cr as a hard mask, SiO₂ and Al₂O₃ layers were removed everywhere except the gate region by reactive ion etching (RIE) and wet etching respectively. The channel was never exposed directly to the RIE. After removal of Cr hard mask using wet etch, a 85 nm thick degenerately doped (1×10^{20} cm⁻³) Ga₂O₃ layer was grown by MOCVD at 700 °C. After regrowth, sample was dipped in buffered HF to remove SiO₂/Al₂O₃ regrowth mask.

Next, device mesa isolation was performed using high power BCl₃ based ICP-RIE etch. Ti/Au/Ni metal stack (50 nm/ 120 nm/ 40 nm) was deposited in the source/drain (S/D) regions by electron-beam evaporation. A 20 nm SiO₂ was deposited using plasma enhanced ALD for gate dielectric followed by a 450 °C 1 minute annealing under N₂ atmosphere to improve the gate oxide quality. SiO₂ was removed from S/D contact regions using low power ICP-RIE etch. Finally, Ni/Au metal (50 nm/270 nm) was patterned to form T-shaped gates. A trilayer resist stack (MMA/PMGI/PMMA) [29] was used for fabricating 160-200 nm foot length and 500 nm top gate hat. The device layout was designed for GSG probing with 2x20 μ m width T-layout.

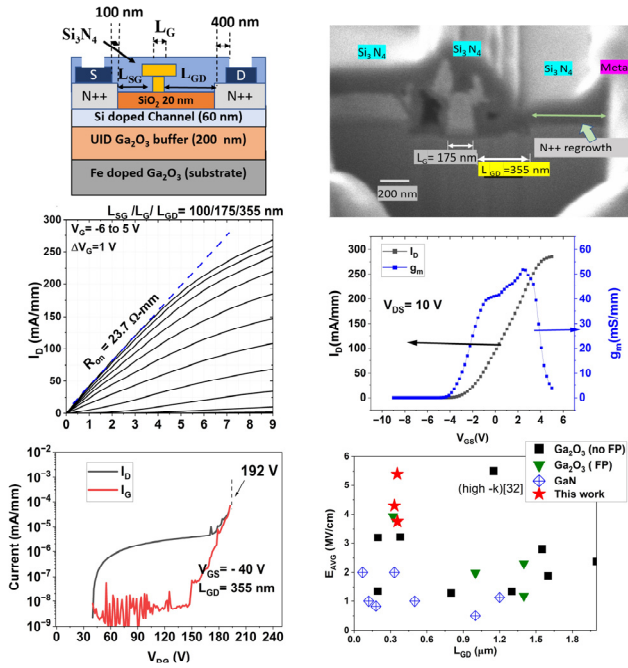


Fig. 1. (a) Cross section schematic of a MOSFET after passivation. (b) FIB-cross section image of a fabricated device after passivation, (c) I_D - V_{DS} output curve and (d) I_D - V_{GS} Transfer curve of the DUT after passivation showing 285 mA/mm on current at $V_{DS} = 10$ V (e) Three terminal off-state breakdown measurement for $L_{GD} = 355$ nm showing breakdown ($V_{DG} = V_{DS} - V_{GS}$) at 192 V. (b) E_{AVG} vs L_{GD} reported in literature with and without Field Plate (FP) technique showing that our device has the highest E_{AVG} among sub-micron devices

The sample was passivated with 200 nm thick Si₃N₄ deposited by PECVD at 250 °C. The Si₃N₄ was removed from the source-drain pad region using CF₄/O₂ based ICP-RIE. The cross section schematic of the device is shown in Fig.1 (a) and a FIB cross section image of a fully passivated device is shown in Fig. 1(b)

III. RESULTS AND DISCUSSION

DC characteristics were measured using 4155B semiconductor parameter analyzer. A 175 nm gate length device gave an on resistance (R_{on}) of 23.7 Ω mm at $V_{GS} = 5$ V (1(c)). Maximum drain current of $I_{DS,MAX} = 285$ mA/mm and peak g_m of 52 mS/mm were recorded at gate bias of 10 V (Fig 1(d)). The peak I_{DS} is comparable to the highest reported current density in gallium oxide FETs [17], [23]. The device shows a depletion mode operation with a threshold voltage of (V_{th}) -4 V. The measured on/off ratio is 1.23×10^5 (not shown) can be further increasing the mesa isolation etch to the substrate. The channel sheet resistance was measured to be 14.2 kΩ/□. A mobility of 80 cm²/V.s is extracted from the measured sheet resistance and calculated sheet charge density. TLMs on the regrowth layer give a low 0.078 Ω mm lateral metal/n⁺ contact resistance with 3.9×10^{-7} Ω cm² specific contact resistance. From TLM measurements, channel sheet resistance data and device dimensions, the n⁺⁺ regrowth/channel interface resistance was estimated to be a high 7.31 Ω mm, contributing to 34% of total on resistance. Atmospheric contaminants at the regrowth interface could be the reason for the high resistance

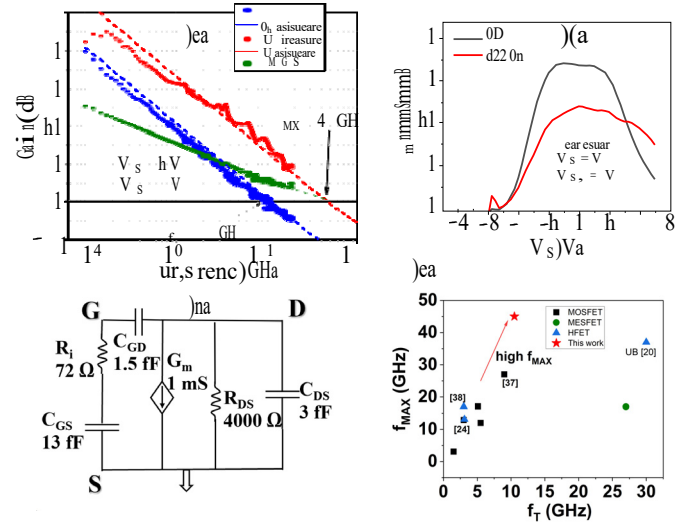


Fig. 2. (a) Measured and simulated small signal RF performance of 175 nm gate length MOSFET showing 48 GHz f_{MAX} (b) small signal equivalent circuit model of our device (c) Pulsed I_D - V_G transfer curve after passivation showing degradation of g_m at 200 nS pulse width (d) f_T vs f_{MAX} plot to benchmark our device with other gallium oxide RF device in literature

as no pre-treatment was carried out before regrowth. Another plausible reason could be the different growth methods of channel layer (MBE) [28] and n⁺⁺ regrown layer (MOCVD) [13], [30]. The different methods use different temperature and different growth conditions. Fully MOCVD grown MESFET has been reported with lower interface resistance and contact resistances [5], [22], [31], which shows that lower interface resistances can be achieved.

Three terminal off state Breakdown measurement was performed on the devices using B1505A power device analyzer. We recorded a breakdown voltage of 152 V (Fig. 1 (e)) at $V_{GS} = -40$ V bias for $L_{GD} = 355$ nm. It corresponds to gate-drain breakdown voltage (V_{BR}) = 192 V and 5.4 MV/cm average breakdown field. This E_{AVG} is the highest reported among β -Ga₂O₃ FETs without using any field engineering [32] for sub-micron length devices [33], [34]. (Fig. 1(f))

High frequency small-signal performance was carried out from 100 MHz to 19 GHz using Keysight ENA 5071C Vector Network Analyzer (VNA). The VNA was calibrated using SOLT technique on sapphire calibration standard. Parasitic pad capacitance was de-embedded using an isolated open-pad device structure on the same wafer. Figure 2(a) shows short circuit current gain (h_{21}), unilateral current gain (U) and maximum available/stable gains (MAG/MSG) at $V_{DS} = 12$ V and $V_{GS} = 1$ V. We extracted current gain cut-off frequency (f_i) of ~ 11 GHz and power gain cut off frequency (f_{MAX}) of approximately ~ 48 GHz. The peak f_{MAX} value is highest reported in β -Ga₂O₃ FETs.

The expected f_T was calculated from the measured DC g_m and calculated C_{GS} [35]. For C_{GS} calculation, half the channel thickness was used. The measured f_T is significantly lower than calculated values (~ 25 GHz) Although the device are passivated and current collapse measured in I_D - V_{DS} was

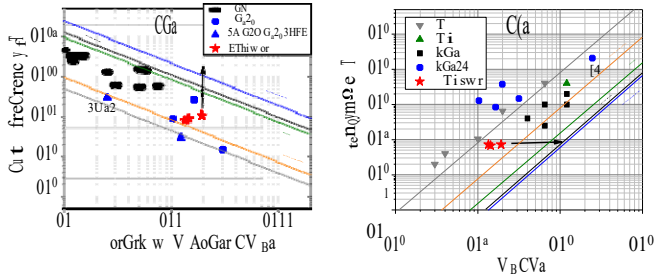


Fig. 3. (a) Johnson's figure of merit showing the trade-off between f_T and maximum operating voltage (V_{BK}) or breakdown voltage (V_{BR}). (b) Huang's Material Figure of merit ($R_{on}\cdot Q_{GD}$ vs. V_{BR}). Materials in the bottom right are considered promising for switching applications

moderately low (<20 %) (not shown). Pulsed I_D - V_G transfer curve shows significant drop of g_m at 200 ns pulse widths (Fig 2 (b)). The source of traps can be attributed to the SiO₂ gate dielectric which is deposited *ex-situ* without any surface treatment. Piranha treatment has been reported to reduce traps and hysteresis in transfer curve and capacitance-Voltage curve [36]. This is in contrast to our previously reported HFET [20], [21] where AlGaO layer was deposited *in-situ* during epitaxial device growth.

We developed a simplified small signal analytical model (Fig 2 (c)) of the MOSFET using Advanced Design System (ADS). In the model, we used the value of reduced pulsed g_m and calculated C_{GS} . The C_{GD} was calculated from the gate-drain separation and measured R_{DS} was used. The R_i was extracted from measured s-parameters at 7 GHz. A good fit is seen between simulated h_{21} and unilateral gain (U) and measured values further confirming the measured RF figures of merit. A scatter plot of f_T vs f_{MAX} previous reported β -Ga₂O₃ devices is shown in (Fig 2 (d)). A f_{MAX}/f_T ratio of 4.3 is obtained because of the T gate structure and record f_{MAX} . Similar f_{MAX}/f_T ratio of 3 to 6 [26], [37], [38] have been reported in literature.

Figure 3 (a) shows the trade off between f_T and V_{br} of different materials. With 11 GHz f_T and 192 V breakdown Voltage, we achieved $f_T \cdot V_{br}$ product of 2.11 THz.V, which is comparable to mature GaN devices. This makes our device a suitable candidate for L band (1-2 GHz) [39] or S band (2-4 GHz) applications with higher operating voltage (V_{br}). Huang's material figure of merit (HMFOM) [40] was calculated by considering that Q_G is dominated by the miller charge Q_{GD} [41]. We estimated Q_{GD} by assuming that full depletion width of the drift region [42], where $Q_{GD} = q \cdot N_D \cdot t_{ch} \cdot L_{GD} \cdot W$. After normalizing with on resistance, we achieved $R_{on} \cdot Q_G$ of 72 m Ω .nC, which surpasses the figure of merit of silicon (Fig. 3(b)) and competitive with SiC and some GaN devices. Similar figure of merit has been reported recently with Ga₂O₃ MESFET [43], but with higher V_{BR} coming from large L_{GD} spacing at the expense of high R_{ON} .

IV. CONCLUSION

In conclusion, we have demonstrated a highly scaled β -Ga₂O₃ T-gate MOSFETs, which shows low R_{ON} and high $I_{DS,MAX}$ and transconductance (g_m) which are comparable

to the state-of-art β -Ga₂O₃ MOSFETs and HFETs. Device shows the highest E_{AVG} for any sub- μ m gate-drain spacing without field plate. We also reported a record $f_{max} = 48$ GHz among β -Ga₂O₃ FETs. Device surpasses switching figure of merit of silicon at $V_{BR} > 100$ V with low $R_{on}\cdot Q_G$ value. RF performance can be further improved using high-k dielectric and better surface treatment at channel-dielectric interface. This process optimization technique with sub-100 nm gate length paves the way for high-power high frequency applications of future Ga₂O₃ MOSFETs

REFERENCES

- [1] A. J. Green, J. Speck, G. Xing, P. Moens, F. Allerstam, K. Gumaelius, T. Neyer, A. Arias-Purdue, V. Mehrotra, A. Kuramata *et al.*, " β -gallium oxide power electronics," *APL Materials*, vol. 10, no. 2, p. 029201, 2022.
- [2] A. J. Green, K. D. Chabak, E. R. Heller, R. C. Fitch, M. Baldini, A. Fiedler, K. Irmscher, G. Wagner, Z. Galazka, S. E. Tetlak, A. Crespo, K. Leedy, and G. H. Jessen, "3.8-mv/cm breakdown strength of movpe-grown sn-doped β -Ga₂O₃ mosfets," *IEEE Electron Device Letters*, vol. 37, no. 7, pp. 902–905, 2016.
- [3] S. Sharma, K. Zeng, S. Saha, and U. Singiseti, "Field-plated lateral Ga₂O₃ mosfets with polymer passivation and 8.03 kv breakdown voltage," *IEEE Electron Device Letters*, vol. 41, no. 6, pp. 836–839, 2020.
- [4] K. Zeng, A. Vaidya, and U. Singiseti, "1.85 kv breakdown voltage in lateral field-plated β -Ga₂O₃," *IEEE Electron Device Letters*, vol. 39, no. 9, pp. 1385–1388, 2018.
- [5] A. Bhattacharyya, P. Ranga, S. Roy, C. Peterson, F. Alema, G. Seryogin, A. Osinsky, and S. Krishnamoorthy, "Multi-kv class β -Ga₂O₃ MESFETs with a lateral figure of merit up to 355 mw/cm²," *IEEE Electron Device Letters*, vol. 42, no. 9, pp. 1272–1275, 2021.
- [6] Z. Hu, K. Nomoto, W. Li, N. Tanen, K. Sasaki, A. Kuramata, T. Nakamura, D. Jena, and H. G. Xing, "Enhancement-mode Ga₂O₃ vertical transistors with breakdown voltage ≥ 1 kv," *IEEE Electron Device Letters*, vol. 39, no. 6, pp. 869–872, 2018.
- [7] J. Zhang, P. Dong, K. Dang, Y. Zhang, Q. Yan, H. Xiang, J. Su, Z. Liu, M. Si, J. Gao, M. Kong, H. Zhou, and Y. Hao, "Ultra-wide bandgap semiconductor Ga₂O₃ power diodes," *Nature communications*, vol. 13, no. 1, pp. 1–8, 2022.
- [8] E. Farzana, F. Alema, W. Y. Ho, A. Mauze, T. Itoh, A. Osinsky, and J. S. Speck, "Vertical β -Ga₂O₃ field plate schottky barrier diode from metal-organic chemical vapor deposition," *Applied Physics Letters*, vol. 118, no. 16, p. 162109, 2021.
- [9] D. H. Mudiyansele, D. Wang, and H. Fu, "Wide bandgap vertical kv-class β -Ga₂O₃/GaN heterojunction pn power diodes with mesa edge termination," *IEEE Journal of the Electron Devices Society*, vol. 10, pp. 89–97, 2021.
- [10] K. Ghosh and U. Singiseti, "Ab initio velocity-field curves in monoclinic β -Ga₂O₃," *Journal of Applied Physics*, vol. 122, no. 3, p. 035702, 2017.
- [11] J. Blewins, K. Stevens, A. Lindsey, G. Foundos, and L. Sande, "Development of large diameter semi-insulating gallium oxide β -Ga₂O₃ substrates," *IEEE Transactions on Semiconductor Manufacturing*, vol. 32, no. 4, pp. 466–472, 2019.
- [12] W. Tang, Y. Ma, X. Zhang, X. Zhou, L. Zhang, X. Zhang, T. Chen, X. Wei, W. Lin, D. H. Mudiyansele, H. Fu, and B. Zhang, "High-quality (001) β -Ga₂O₃ homoepitaxial growth by metalorganic chemical vapor deposition enabled by in situ indium surfactant," *Applied Physics Letters*, vol. 120, no. 21, p. 212103, 2022.
- [13] Z. Feng, A. Anhar Uddin Bhuiyan, M. R. Karim, and H. Zhao, "Mocvd homoepitaxy of si-doped (010) β -Ga₂O₃ thin films with superior transport properties," *Applied Physics Letters*, vol. 114, no. 25, p. 250601, 2019.
- [14] K. Sasaki, A. Kuramata, T. Masui, E. G. Villora, K. Shimamura, and S. Yamakoshi, "Device-quality β -Ga₂O₃ epitaxial films fabricated by ozone molecular beam epitaxy," *Applied Physics Express*, vol. 5, no. 3, p. 035502, 2012.
- [15] X. Tang, K.-H. Li, C.-H. Liao, D. Zheng, C. Liu, R. Lin, N. Xiao, S. Krishna, J. Tauboda, and X. Li, "Epitaxial growth of β -Ga₂O₃ (201) thin film on four-fold symmetry CeO₂ (001) substrate for heterogeneous integrations," *Journal of Materials Chemistry C*, vol. 9, no. 44, pp. 15868–15876, 2021.

- [16] C.-H. Jang, G. Atmaca, and H.-Y. Cha, "Normally-off β -Ga₂O₃ mosfet with an epitaxial drift layer," *Micromachines*, vol. 13, no. 8, p. 1185, 2022.
- [17] C. Wang, H. Zhou, J. Zhang, W. Mu, J. Wei, Z. Jia, X. Zheng, X. Luo, X. Tao, and Y. Hao, "Hysteresis-free and μ s-switching of D/E-modes β -Ga₂O₃ hetero-junction FETs with the BV²/Ron, sp of 0.74/0.28 GW/cm²," *Applied Physics Letters*, vol. 120, no. 11, p. 112101, 2022.
- [18] P. Kachhawa and N. Chaturvedi, "A simulation approach for depletion and enhancement mode in β -Ga₂O₃ mosfet," *IETE Technical Review*, pp. 1–9, 2021.
- [19] K. D. Chabak, J. P. McCandless, N. A. Moser, A. J. Green, K. Mahalingam, A. Crespo, N. Hendricks, B. M. Howe, S. E. Tetlak, K. Leedy, R. C. Fitch, D. Wakimoto, K. Sasaki, A. Kuramata, and G. H. Jessen, "Recessed-gate enhancement-mode β -Ga₂O₃ mosfets," *IEEE Electron device letters*, vol. 39, no. 1, pp. 67–70, 2017.
- [20] A. Vaidya, C. N. Saha, and U. Singiseti, "Enhancement mode β -(Al_xGa_{1-x})₂O₃/Ga₂O₃ heterostructure fet (hfet) with high transconductance and cutoff frequency," *IEEE Electron Device Letters*, vol. 42, no. 10, pp. 1444–1447, 2021.
- [21] C. N. Saha, A. Vaidya, and U. Singiseti, "Temperature dependent pulsed iv and rf characterization of β -(Al_xGa_{1-x})₂O₃/Ga₂O₃ hetero-structure FET with ex situ passivation," *Applied Physics Letters*, vol. 120, no. 17, p. 172102, 2022.
- [22] A. Bhattacharyya, S. Roy, P. Ranga, D. Shoemaker, Y. Song, J. S. Lundh, S. Choi, and S. Krishnamoorthy, "130 ma mm⁻¹ β -Ga₂O₃ metal semiconductor field effect transistor with low-temperature metalorganic vapor phase epitaxy-regrown ohmic contacts," *Applied Physics Express*, vol. 14, no. 7, p. 076502, 2021.
- [23] Z. Xia, H. Xue, C. Joishi, J. Mcglone, N. K. Kalarickal, S. H. Sohel, M. Brenner, A. Arehart, S. Ringel, S. Lodha, W. Lu, and S. Rajan, " β -Ga₂O₃ delta-doped field-effect transistors with current gain cutoff frequency of 27 GHz," *IEEE Electron Device Letters*, vol. 40, no. 7, pp. 1052–1055, 2019.
- [24] Y. Zhang, A. Neal, Z. Xia, C. Joishi, J. M. Johnson, Y. Zheng, S. Bajaj, M. Brenner, D. Dorsey, K. Chabak, G. Jessen, J. Hwang, S. Mou, J. P. Heremans, and S. Rajan, "Demonstration of high mobility and quantum transport in modulation-doped β -(Al_xGa_{1-x})₂O₃ heterostructures," *Applied Physics Letters*, vol. 112, no. 17, p. 173502, 2018.
- [25] A. Vaidya and U. Singiseti, "Temperature-dependent current dispersion study in β -Ga₂O₃ fets using submicrosecond pulsed i-v characteristics," *IEEE Transactions on Electron Devices*, vol. 68, no. 8, pp. 3755–3761, 2021.
- [26] A. J. Green, K. D. Chabak, M. Baldini, N. Moser, R. Gilbert, R. C. Fitch, G. Wagner, Z. Galazka, J. McCandless, A. Crespo, K. Leedy, and G. H. Jessen, " β -Ga₂O₃ mosfets for radio frequency operation," *IEEE Electron Device Letters*, vol. 38, no. 6, pp. 790–793, 2017.
- [27] X. Yu, H. Gong, J. Zhou, Z. Shen, F.-f. Ren, D. Chen, X. Ou, Y. Kong, Z. Li, T. Chen, S. Gu, R. Zhang, Y. Zheng, and J. Ye, "Rf performance enhancement in sub- μ m scaled β -Ga₂O₃ tri-gate finfets," *Applied Physics Letters*, vol. 121, no. 7, p. 072102, 2022.
- [28] A. Vaidya, J. Sarker, Y. Zhang, L. Lubecki, J. Wallace, J. D. Poplawsky, K. Sasaki, A. Kuramata, A. Goyal, J. A. Gardella, and U. Singiseti, "Structural, band and electrical characterization of β -(Al_{0.19}Ga_{0.81})₂O₃ films grown by molecular beam epitaxy on sn doped β -Ga₂O₃ substrate," *Journal of Applied Physics*, vol. 126, no. 9, p. 095702, 2019.
- [29] K.-S. Lee, Y.-S. Kim, Y.-K. Hong, and Y.-H. Jeong, "Fabrication of 35-nm zigzag t-gate Al_{0.25}Ga_{0.75}As/In_{0.2}Ga_{0.8}As/GaAs pHEMTs," in *2006 IEEE Nanotechnology Materials and Devices Conference*, vol. 1. IEEE, 2006, pp. 112–113.
- [30] H. Ghadi, J. F. McGlone, Z. Feng, A. A. U. Bhuiyan, H. Zhao, A. R. Arehart, and S. A. Ringel, "Influence of growth temperature on defect states throughout the bandgap of mcvd-grown β -Ga₂O₃," *Applied Physics Letters*, vol. 117, no. 17, p. 172106, 2020.
- [31] A. Bhattacharyya, S. Roy, P. Ranga, C. Peterson, and S. Krishnamoorthy, "High-mobility tri-gate β -Ga₂O₃ MESFETs with a power figure of merit over 0.9 GW/cm²," *IEEE Electron Device Letters*, vol. 43, no. 10, pp. 1637–1640, 2022.
- [32] N. K. Kalarickal, Z. Xia, H.-L. Huang, W. Moore, Y. Liu, M. Brenner, J. Hwang, and S. Rajan, " β -(Al_{0.18}Ga_{0.82})₂O₃ double heterojunction transistor with average field of 5.5 mv/cm," *IEEE Electron Device Letters*, vol. 42, no. 6, pp. 899–902, 2021.
- [33] Y. Zhang, C. Joishi, Z. Xia, M. Brenner, S. Lodha, and S. Rajan, "Demonstration of β -(Al_xGa_{1-x})₂O₃/Ga₂O₃ hetero-structure FET double heterostructure field effect transistors," *Applied physics letters*, vol. 112, no. 23, p. 233503, 2018.
- [34] C. Joishi, Y. Zhang, Z. Xia, W. Sun, A. R. Arehart, S. Ringel, S. Lodha, and S. Rajan, "Breakdown characteristics of β -(Al_{0.22}Ga_{0.78})₂O₃ field-plated modulation-doped field-effect transistors," *IEEE Electron Device Letters*, vol. 40, no. 8, pp. 1241–1244, 2019.
- [35] P. J. Tasker and B. Hughes, "Importance of source and drain resistance to the maximum f/sub t/of millimeter-wave modfets," *IEEE Electron Device Letters*, vol. 10, no. 7, pp. 291–293, 1989.
- [36] A. Islam, K. D. Leedy, N. A. Moser, S. Ganguli, K. J. Liddy, A. J. Green, and K. D. Chabak, "Hysteresis-free moscap made with Al₂O₃/(010) β -Ga₂O₃ interface using a combination of surface cleaning, etching and post-deposition annealing," in *2021 Device Research Conference (DRC)*. IEEE, 2021, pp. 1–2.
- [37] T. Kamimura, Y. Nakata, and M. Higashiwaki, "Delay-time analysis in radio-frequency β -Ga₂O₃ field effect transistors," *Applied Physics Letters*, vol. 117, no. 25, p. 253501, 2020.
- [38] Y. Zhang, Z. Xia, J. Mcglone, W. Sun, C. Joishi, A. R. Arehart, S. A. Ringel, and S. Rajan, "Evaluation of low-temperature saturation velocity in β -(Al_xGa_{1-x})₂O₃/Ga₂O₃ modulation-doped field-effect transistors," *IEEE Transactions on Electron Devices*, vol. 66, no. 3, pp. 1574–1578, 2019.
- [39] F. J. Ortega-Gonzalez, D. Tena-Ramos, M. Patiño-Gomez, J. M. Pardo-Martin, and D. Madueño-Pulido, "High-power wideband l-band suboptimum class-e power amplifier," *IEEE transactions on microwave theory and techniques*, vol. 61, no. 10, pp. 3712–3720, 2013.
- [40] A. Q. Huang, "New unipolar switching power device figures of merit," *IEEE Electron Device Letters*, vol. 25, no. 5, pp. 298–301, 2004.
- [41] D. Reusch and J. Strydom, "Evaluation of gallium nitride transistors in high frequency resonant and soft-switching dc-dc converters," *IEEE Transactions on Power Electronics*, vol. 30, no. 9, pp. 5151–5158, 2014.
- [42] Y. Zhang, M. Sun, J. Perozek, Z. Liu, A. Zubair, D. Piedra, N. Chowdhury, X. Gao, K. Shepard, and T. Palacios, "Large-area 1.2-kv GaN vertical power finfets with a record switching figure of merit," *IEEE Electron Device Letters*, vol. 40, no. 1, pp. 75–78, 2018.
- [43] D. M. Dryden, K. J. Liddy, A. E. Islam, J. C. Williams, D. E. Walker, N. S. Hendricks, N. A. Moser, A. Arias-Purdue, N. P. Sepelak, K. DeLello *et al.*, "Scaled t-gate β -Ga₂O₃ mesfets with 2.45 kv breakdown and high switching figure of merit," *IEEE Electron Device Letters*, vol. 43, no. 8, pp. 1307–1310, 2022.